Chapter 37
Structural Health Monitoring Based on Guided Waves

**Daniel Schmidt, Wolfgang Hillger, Artur Szewieczek
and Michael Sinapius**

Abstract Structural Health Monitoring (SHM) based on ultrasonic guided waves, so-called Lamb waves, is a promising method for in-service inspection of composite structures without time consuming scanning like conventional ultrasonic techniques. Lamb waves are able to propagate over large distances and can be easily excited and received by a network of piezoelectric actuators and sensors. In principle different kinds of structural defects can be detected and located by analyzing the sensor signals. The chapter describes recent research activities at DLR on Structural Health Monitoring. The research are focused on the visualisation of Lamb wave propagation fields based on air-coupled ultrasonic technique, the simulation of virtual sensors, mode selective actuators as well as manufacturing of actuator and sensor networks. Additionally, the chapter present the development of a SHM system for impact detection in a helicopter tailboom (Eurocopter—EC 135).

D. Schmidt (✉) · W. Hillger · A. Szewieczek · M. Sinapius
Institute of Composite Structures and Adaptive Systems, German Aerospace Center DLR,
Lilienthalplatz 7, 38108, Braunschweig, Germany
e-mail: daniel.schmidt@dlr.de

W. Hillger
e-mail: wolfgang.hillger@dlr.de

A. Szewieczek
e-mail: artur.szewieczek@dlr.de

M. Sinapius
e-mail: michael.sinapius@dlr.de

37.1 Introduction

Structural Health Monitoring (SHM) based on ultrasonic guided waves, so-called Lamb waves, is a promising method for in-service inspection of aerospace structures without time consuming scanning like conventional ultrasonic techniques. The implementation of SHM systems into aerospace applications enhances reliability, safety and maintenance performance as well as economic aspects. Lamb waves are disperse guided waves which propagate between two parallel surfaces, e.g. the upper and lower plate surface. Due to the disperse characteristic, the wave velocity depends on the product of excitation frequency and plate thickness. At a given frequency-thickness product a finite number of different Lamb wave modes (symmetric, S_0, S_1, S_2,…, and anti-symmetric, A_0, A_1, A_2,…, modes) exist [1, 2].

Lamb waves are able to propagate over long distances in thin-walled structures with low attenuation and are highly sensitive to a variety of structural damages [3–6].

Lamb waves are best excited and received using a network of piezoelectric actuators and sensors which are permanently attached on the structure. Piezopolymers, like polyvinylidene fluoride (PVDF), or piezoceramics (PZT) are commonly used as actuator and sensor materials for Lamb wave based Structural Health Monitoring. Piezopolymers are flexible and can be applied on curved structures. They are lightweight as well as cheaper and easier to manufacture than piezoceramics [7]. However, piezopolymers possess a much lower Young's modulus and actuation force in comparison to piezoceramics. Thus piezopolymers are less suitable as actuators. Moreover, piezopolymers are inappropriate for aerospace applications due to their limited temperature range of −40 to +110°C. Hence, the presented work is focused on piezoceramic based Structural Health Monitoring.

Different kinds of structural defects can be detected in principle and located by analysing the sensor signals of guided Lamb waves [8, 9]. However, the presence of at least two Lamb wave modes at any given frequency, their dispersive characteristic and their interference at structural discontinuities produce complex wave propagation fields and sensor signals which are difficult to evaluate. Furthermore, discrete sensors provide only point information. An understanding of the complete wave propagation is not derivable out of these sensor signals. Therefore it is necessary to visualize the wave propagation in order to get a profound understanding of the propagation of different Lamb wave modes and their individual interaction with defects. Usually this is done by scanning laser vibrometry [10]. DLR has developed a method using air-coupled ultrasonic scanning technique, which is presented in the next section. The third section describes the design and positioning of virtual sensors based on the scanned wave propagation field. By using this method different sensor layouts and positions can be compared and evaluated in order to optimize SHM systems. Mode selective actuators are able to excite a particular Lamb wave mode to

Fig. 37.1 Experimental set-up for lamb wave investigations based on air-coupled ultrasonic technique
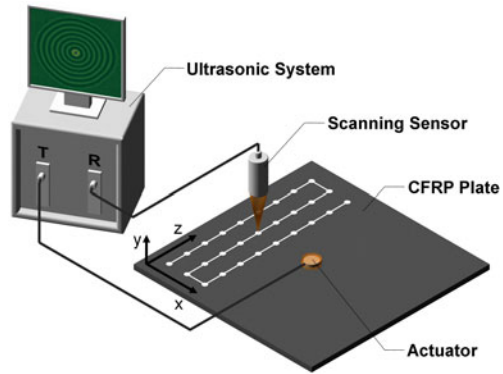
reduce the complexity of the wave propagation field. Section 37.4 describes the development and the manufacturing of mode selective actuators. The experimental validation of the mode selective actuators is elucidated thru experiments on a CFRP (Carbon Fiber Reinforced Plastics) plate. Finally, a SHM system for impact detection in a helicopter tailboom (Eurocopter—EC 135) is proposed in Sect. 37.5.

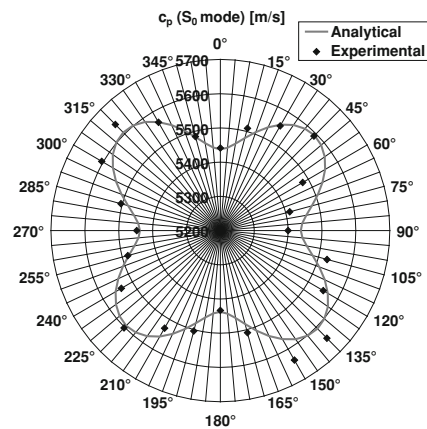## 37.2 Visualisation of the Lamb Wave Propagation Field

Air-coupled ultrasonic technique is a well-established method at DLR for the inspection of CFRP structures. This technique has been combined with Lamb wave investigations in order to visualize the Lamb wave propagation field and its interaction with defects. Figure 37.1 shows the experimental set-up used for visualization of Lamb wave propagation fields.

A piezoceramic actuator is applied in the set-up on the lower surface of the specimen and operates as transmitter. A rectangle burst signal is used for excitation. Due to the harmonics of the rectangular signal the receiver signal is filtered in order to provide a narrow band signal. An air-coupled ultrasonic sensor is moved in a meander-shaped track by a portal scanner for receiving the out-of-plane component of the Lamb wave propagation field. Broadband capacitive sensors providing a frequency range from 10 to 100 kHz can also be utilized in addition to ultrasonic sensors having a relative narrowband characteristic with centre frequencies of e.g. 120, 200, 300 and 400 kHz. The amplitudes of the receiver signal are very low due to the air-coupling of the sensors and the mode conversion into longitudinal waves. In consequence, ultra-low noise preamplifiers and a band pass filter on the receiver side are required. The amplitude signal as a function of time [A = f(t)] is measured during the scanning process at each point in x- and y-direction of the scanning grid. Depending on the x- and y-coordinates the amplitude signals are recorded into a so-called volume data file [A = f(x,y,t)].

Fig. 37.2 Phase velocity of
A_0 mode in x–y plane,
131 kHz, 2 mm thick CFRP
plate
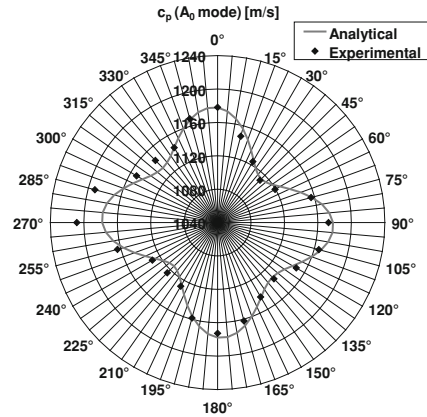
Fig. 37.3 Phase velocity of
S_0 mode in x–y plane,
131 kHz, 2 mm thick CFRP
plate

This volume data file contains the entire information of the Lamb wave propa-
gation field so that several analysis tools can be calculated:

- A-scan, amplitude signal as a function of time at specific x–y-positions
- B-scan, amplitude signal as a function of time along an axis in x–y-plane
- C-scan, two dimensional image of maximal amplitudes
- D-scan, two dimensional image of time-of-flight
- Video animation of the wave propagation

   Further analysis tools provide the measurement of specific Lamb wave modes
regarding wavelength, phase and group velocity as well as signal attenuation. This
measurement can be performed in different angles of the x–y-plane which is
fundamental for the characterisation of anisotropic structures, such as CFRP.
   Within the investigations the phase velocities of the A_0 and S_0 mode in a CFRP
plate are experimentally determined by air-coupled ultrasonic technique. The

CFRP plate have dimensions of $1000 \times 1000 \times 2$ mm and are made of [7] plies in a $[(0/90)_f/+45/-45/(0/90);_f]_S$ configuration. The experimentally determined phase velocities of A_0 and S_0 mode at 131 kHz are shown in Figs. 37.2 and 37.3. In these figures the experimental measurements are compared with the theoretical phase velocities which are determined by the method of guided waves in multiple layers proposed in [9] and [11]. In addition, the phase velocities of the CFRP plates were measured using scanning laser vibrometry which was performed by the Otto von Guericke University of Magdeburg-Germany [12]. The scanning laser vibrometry as well as the ultrasonic technique are appropriate for measurement the dispersion diagram with the same accuracy. Figures 37.2 and 37.3 show that the phase velocity also depends on the direction of propagation in the x–y plane. It can be seen, that the phase velocity pattern is different between A_0 and S_0 mode. This is caused by the lay-up of the CFRP plate which leads to varying stiffnesses in different directions and thicknesses. The varying stiffness of the CFRP plate in combination with the complex displacement field of the Lamb wave modes results in different phase velocity pattern. For instance, the displacement field across the thickness of the A_0 mode resemble for low frequencies ($fd \rightarrow 0$) a conventional flexure wave. In contrast, the displacement field of the S_0 mode resemble for low frequencies ($fd \rightarrow 0$) a conventional axial plate wave [8].

37.3 Virtual Design and Evaluation of Sensors

The volume data file described in chap. 37.2 includes the entire information of the wave propagation field for a chosen excitation frequency. This volume data can be used in combination with structure information to simulate the signal of a sensor with known dimensions and behaviour as if it would be bonded on the structure surface. In this way it is possible to optimize the sensor design and network configuration (number of sensors and their positions) with higher time and cost efficiency [13].

After defining the coordinated of the virtual sensor within a wave propagation snapshot, the software calculates the anticipated signal of an equivalent sensor by analysing the volume data file. Every imaginable layout can be simulated. The software considers different coupling techniques and sensor layouts. Figure 37.4 shows an investigation of simulated sensors with an interdigital transducer layout for mode selection 0, [14]. An aluminium plate with the dimensions of $1000 \times 1000 \times 2$ mm was used for experimental verification. A circular piezoceramic actuator having a diameter of 10 mm and a thickness of 0.5 mm was bonded on the plate centre. The actuator is excited by a rectangle burst signal with a frequency of 120 kHz. The Lamb wave propagation field is recorded with the air-coupled ultrasonic scanning technique, as presented above. The wave propagation field is shown in Fig. 37.4 for two different points of time (152.2 and 200 μs). The wavelengths of the excited Lamb wave modes are
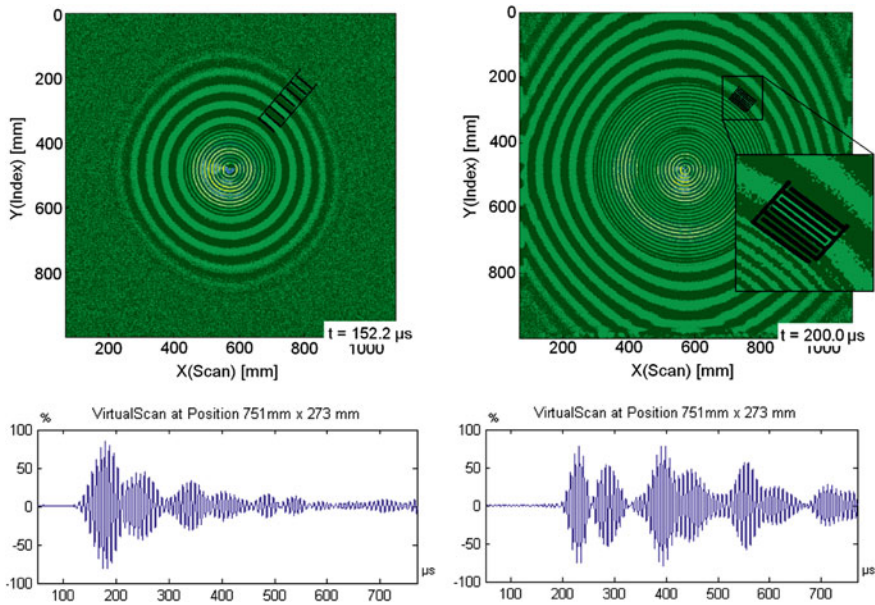
Fig. 37.4 Snapshots of lamb wave propagation field in an aluminium plate with different. virtual sensors (*left* S_0 mode, *right* A_0 mode) and their calculated signals

measured with the in-house developed analysis software. The procedure of the wavelength measurement is detailed described in [12]. The results show that the S_0 mode propagates with a wavelength of 49 mm and the A_0 mode propagates with a wavelength of 13 mm.

Two different virtual sensors are designed in the simulation according to the wavelengths of S_0 mode (Fig. 37.4—left) and A_0 mode (Fig. 37.4—right). The width of each sensor is 60 mm. As a result of the simulation the calculated signals in Fig. 37.4 show a high separation of both Lamb wave modes at the time of arriving at the sensor positions.

37.4 Mode Selective Actuator Design and Manufacturing Process

The generation of a particular Lamb wave mode can be achieved by controlling the frequency as well as the wavelength (λ) of the desired mode within the excitation. An appropriate technical solution is to use piezoelectric substrate with applied interdigitated electrode pattern, so-called interdigital transducers [7, 14, 15]. Such transducers are widespread in telecommunication systems as surface acoustic wave filters (SAW) for frequency selection [16]. The electrode configuration is made of two comb-like electrodes with opposite polarity. The electrode distance

Fig. 37.5 Schematic design of an IDT with apodization
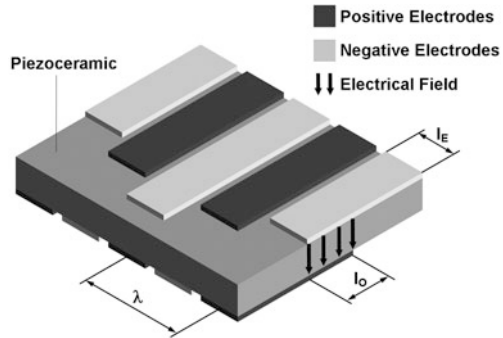
corresponds to the half-wavelength of the desired Lamb wave mode which will be excited at a frequency in the thin-walled structure. The bandwidth of the frequency response function of the excited Lamb wave can be controlled by the number of electrodes. Furthermore, the frequency response function can be modified by apodization which is known from the theory of surface acoustic wave filters. Apodization means that the overlaps (l_O) of each electrode pair are varying along the length of the transducer (Fig. 37.5). By suitable dimensioning of the overlaps the transducer can be in principle designed to a specific frequency response. These possibilities of modifying the frequency response function can be utilized to enhance the effectiveness of the actuator regarding mode selectivity.

Starting point for the manufacturing of interdigital transducer is a commercial available piezoceramic plate with a typical thickness of 0.2–0.5 mm. This piezoceramic plate is already provided with uniform electrodes on the upper and lower surface and polarized by the manufacturer. In a first step the piezoceramic plate is additionally metallised with gold by a sputtering process. This procedure ensures wrap-around electrodes and thus the electrical connection from the upper side of the final actuator. In a second step the electrode structure is made by a laser ablation process. The laser parameters are adjusted to remove only the metallised layer and avoid mechanical damages of the piezoceramic. Due to the polarisation direction and the electrical field, which is generated through the thickness of the piezoceramic, the transducer is working in the piezoelectric d_{31}-effect. In this case a positive electrical field causes in-plane contraction of the piezoceramic material which is used for Lamb wave excitation. A typical example of such an interdigital transducer is shown in Fig. 37.6.

The main problems of piezoceramics are their inherent brittleness and the failures of electrical contacts which lead to insufficient reliability. A promising alternative to conventional piezoceramics is to utilize the piezocomposite technology to increase the reliability of brittle piezoceramics. Piezocomposites consist of piezoceramic materials embedded in a ductile polymer. Further components like electrodes, electrical contacts or insulators are also embedded into the composite. Within the embedding process the polymer is typically cured in a temperature range of 120–180°C. Due to the different coefficients of thermal expansion of the
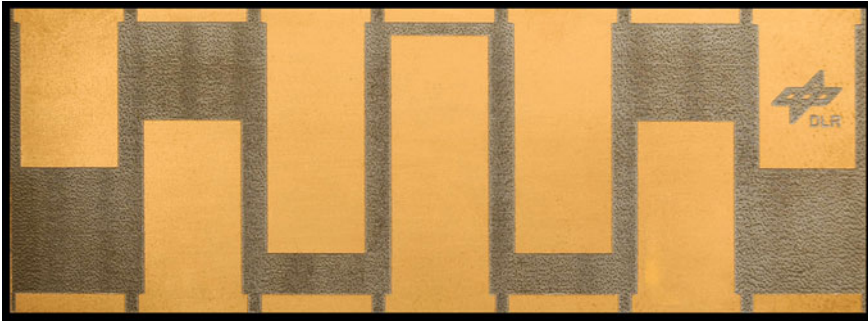
Fig. 37.6 Mode selective lamb wave actuator based on interdigital transducer design with apodization

**Fig. 37.7** Mode selective lamb wave actuators based on piezocomposite technology
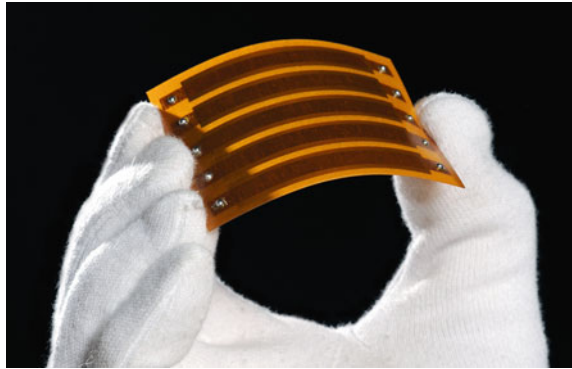
polymer and the piezoceramic material as well as to the shrinking of the polymer during curing, the piezoceramic material is provided with a mechanical pre-compression. This pre-compression protects the brittle piezoceramic material and allows bending loads on the piezocomposite which is essential for the application on curved structures. Further advantages of piezocomposites are reliable electrical contacts, electrical insulation as well as high durability under variable environments. In recent years different piezocomposite configurations have been designed and manufactured [17].

One possible solution of manufacturing mode selective actuators based on the piezocomposite technology is the embedding of the piezoceramic with interdigitated electrode pattern, which is shown in Fig. 37.6, into the polymer. Another solution is to arrange individual piezoceramic elements in a distance of half-wavelength within the piezocomposite (Fig. 37.7). The piezoceramic elements work in the piezoelectric d_{31}-effect.

For experimental tests a mode selective actuator is designed and manufactured. The actuator is designed to attenuate the S_0 mode and thus to amplify the A_0 mode at a frequency of 40 kHz. At this frequency only the lowest order of symmetric

Fig. 37.8 Experimental set-up and sensor signal by driving the first element of the actuator
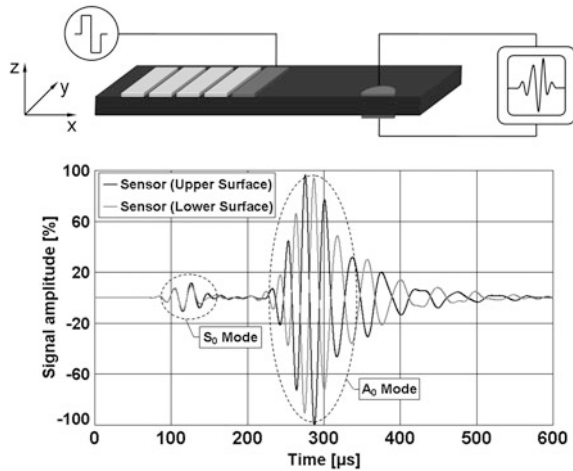
and anti-symmetric modes exists which is a first reduction of the complex Lamb wave propagation field. Due to the dispersion diagram of the CFRP plate the wavelength of the A_0 mode at 40 kHz is approx. 20 mm. The actuator is manufactured as piezocomposite and consists of five piezoceramic elements which have respective dimensions of $50 \times 8 \times 0.2$ mm. The distance between the elements corresponds to the half-wavelength of 10 mm. The final actuator that is used for the experimental tests is shown in Fig. 37.7. The actuator is bonded in $0°$-direction on the upper surface of the CFRP plate which is presented in Sect. 37.2. As bonding layer a cyanoacrylate adhesive is used. Due to the low viscosity of the uncured adhesive very thin and uniform bonding layers can be ensured. Each actuator element is excited by a rectangle burst signal with 3 bipolar pulses, whereby the signal of adjacent elements has a $180°$ phase difference. The voltage of the excitation signal is 15 V (peak to peak). In order to distinguish the S_0 mode from the A_0 mode a pair of circular piezoceramic sensors is collocated bonded on the upper and lower plate surface. In case of the symmetric S_0 mode both sensors show equal amplitude signals over time without a phase shift. But in case of the anti-symmetric A_0 mode the amplitude signals of the upper and lower sensor show a $180°$ phase shift. The sensors are piezocomposites with an embedded circular piezoceramic which has a diameter of 10 mm and a thickness of 0.2 mm. The distance between the actuator and the sensors is set to 200 mm. The sensor signals are filtered using a 12th order band pass of 20–60 kHz. The amplitudes are measured building the absolute value of the signal of each Lamb wave mode. In a first setup only the first element of the actuator is driven. The sensor signals in Fig. 37.8 shows that the A_0 and the S_0 mode are generated in an amplitude ratio of 100 to 11%.

In a second setup all elements of the actuator are driven. The resulting amplitude ratio is 100% of the A_0 mode to 1.7% of the S_0 mode. The amplitude ratio can be improved by applying an apodization. This is realized by controlling the voltage of the excitation signal of each actuator element using adjustable

Fig. 37.9 Experimental set-up and sensor signal by driving all elements of the actuator with applied apodization
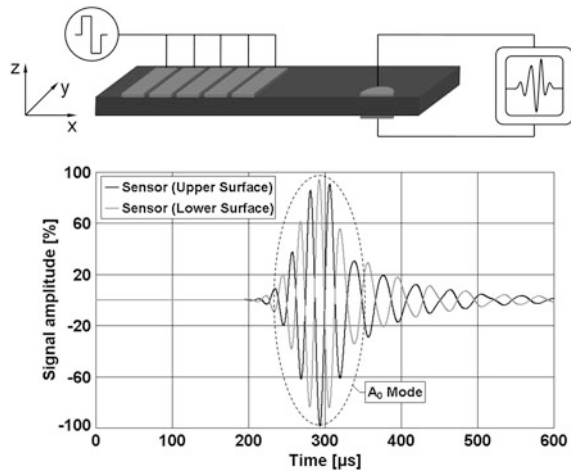
resistors. The apodization is set in such a way that the S_0 mode shows minimal amplitudes over the frequency bandwidth of the sensor signal. The aim of the apodization is to modify the frequency response functions of the S_0 mode as well as the A_0 mode so that a broadband reduction of the S_0 mode is achieved. Figure 37.9 shows the signal amplitudes of the apodized actuator. The signal amplitude of the S_0 mode is reduced to 0.2% in contrast to the amplitude of the A_0 mode of 100%. As a result, the experimental tests show that he designed actuator can be sufficiently attenuated the S_0 mode in a CFRP plate. Furthermore, an apodization modifies the frequency response of the actuators in such a way that the mode selectivity can be improved.

## 37.5 Concept of Damage Detection in a Helicopter Tailboom

Bridging the gap between basic research and application DLR's research on SHM covers the investigation of a SHM system on a half-shell of the EC 135 helicopter tailboom. The research is focused on the ability of defect detection in the helicopter tailboom. Figure 37.10 shows the half-shell of the tailboom (3.49 × 0.57 m).

The tailboom consists of a honeycomb sandwich structure (skin thicknesses 1.0 and 0.5 mm) with copper mesh in the outer skin for lightning protection and different inserts. The wave propagation in such sandwich structure is quite complex. Therefore the wave propagation is visualized using the air-coupled ultrasonic scanning technique which is presented in Sect. 37.2.

Initial experiments reveal that only excitation at frequencies below 30 kHz generate wave modes which propagate in both skins and in the sandwich core. This aspect is important because the actuator and sensor system is applied on the inner skin and must also be able to detect damages in the outer skin as well as in the core.

Fig. 37.10 Tailboom (half-shell) of Eurocopter EC 135
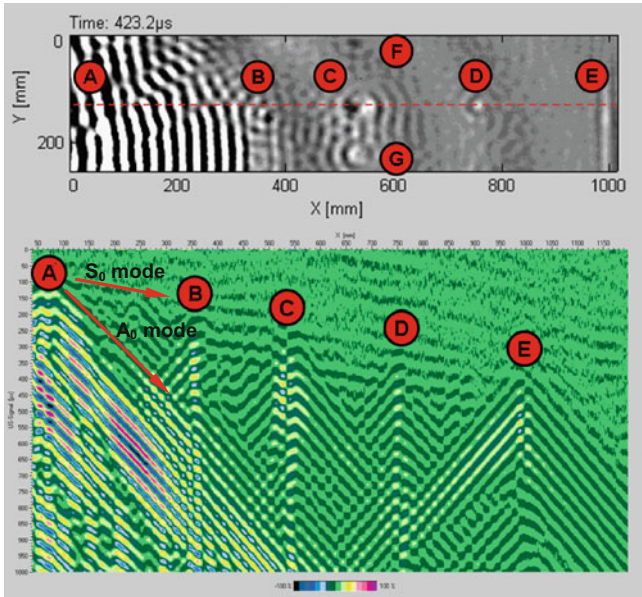
Fig. 37.11 Snapshot of the wave propagation in the tailboom (*top*), B-scan along the red dashed line in the snapshot (*bottom*)

In order to study the wave interaction with an impact and applied piezoceramic sensors, the wave propagation in the tailboom has been recoded over a length of 1 m. Figure 37.11 shows the wave propagation in the tailboom. The actuator is situated at point (A) and excites the S- and the A-mode. At position (B), (D), (F) and (G) circular piezoceramic sensor (PIC 255, Ø 10 × 0.2 mm, PI Ceramic GmbH) are bonded on the inner skin. At position (C) an impact with energy of 10 J is applied on the outer skin. Position (E) indicates a separation of the sandwich core. It can be seen that every stiffness change, like sensors, impacts and core separations, produce mode conversion from the S-mode into the A-mode. Based on the wave propagation these stiffness changes behave like virtual A-mode sources. This means the more sensors required for precise defect detection and localisation, the more additional mode conversions appear.

Fig. 37.12 Air-coupled
sensors are used for the
sensor network
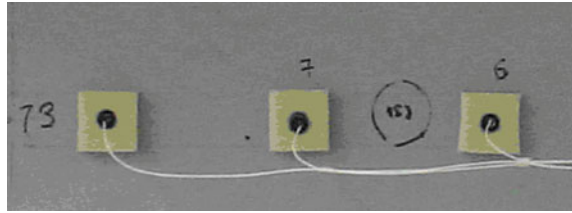
Based on the results of the wave propagation a concept of damage detection in
the tailboom has been developed. This concept uses mode conversion as an
indicator for damages. In order to have a minimal additional distortion of the wave
propagation only few actuators should be applied on the structure. This is possible
because Lamb waves propagate over large distances with low attenuation. The
actuators should be optimised for the S0-mode with a wavelength 185 mm at
22 kHz. Interdigital actuators, as is presented in Sect. 37.4, provide a wavelength
selection. However, their dimensions are too large for this application requiring a
wavelength of 185 mm.

Because of the mode conversions at glued actuators they should be position at
"natural stiffness changes" of the tailboom. Those positions are internal core
bondings in a distance of about 1 m.

In order to avoid additional mode conversion air-coupled sensor networks are
used. These kinds of sensors are sensitive to the out-of-plane component of Lamb
waves. Low frequencies between 20 and 30 kHz generate Lamb waves with higher
out-of-plane components of the A-mode than the S-mode which is another
advantage of the air-coupled system (Fig. 37.12).

Integrated SHM networks underlie different kinds of electromagnetic pertur-
bation. A high signal to noise ratio of the measurements requires an optimized
signal processing and cable design. On the other hand complex cabling of entire
networks accompanies with a high system weight. A weight-saving solution is a
tree-like organisation of multiplexer entities. Local groups of sensors can be
connected to a multiplexer. Different multiplexers can be arranged together in
dependence of the network layout for minimal cable usage. The aim is a solution
as simple as possible with a minimum of (shielded) cables from the SHM system
to the tailboom. A standard VGA monitor cable contains three shielded coax
cables (75 Ω) and ten control lines and is easily deliverable up to a length of 10 m.
The actuators are multiplexed by relays so that only one internal coax cable is
required. The 64 sensors are segmented in eight sensor arrays, each with eight
selected sensors (Fig. 37.13). The eight sensors of an array are connected to the
sensor multiplexer. Its output is amplified by a low noise pre-amplifier and con-
nected to an array multiplexer so that only one coax cable connection to the SHM
system is necessary. A DC coupled technique between sensors, multiplexers and
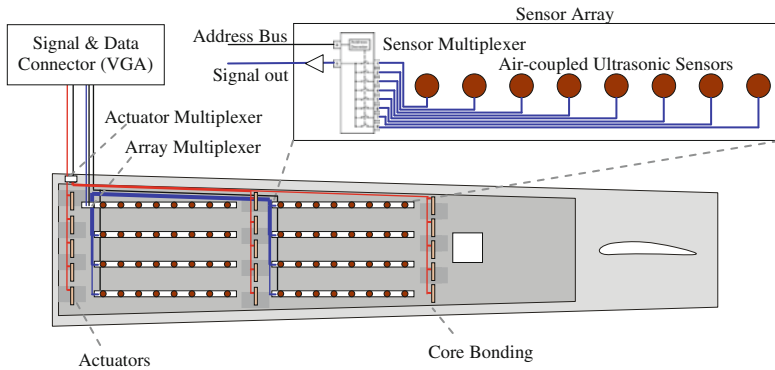amplifiers is used so that only a single supply is necessary.

Fig. 37.13 SHM system of the helicopter tailboom

37.6 Conclusion

Structural Health Monitoring based on Lamb waves is a promising technology for in-service inspection of aerospace structures. For the design of SHM systems in respect to different application requirements the visualisation of the wave propagation field is essential. As presented, the air-coupled ultrasonic scanning technique is a suitable methodology for this task, especially the recording of the complete wave propagation field by volume data files. These data files in combination with different analysis tools provide the basis for the design of actuators, sensors, signal processing and algorithms for damage detection. It has been shown that the signal of virtual sensors can be simulated using the scanned propagation field. It could be demonstrated that mode selective actuators are able to excite a particular Lamb wave mode in a CFRP plate. The design and manufacturing of reliable actuator and sensor networks are presented. Finally, a concept of damage detection in a helicopter tailboom has been shown.

References

1. Viktorov, I.A.: Rayleigh and Lamb Waves: Physical Theory and Applications. Plenum Press, New york (1967)
2. Achenbach, J.D.: Wave Propagation in Elastic Solids. North-Holland Publishing Company, Amsterdam (1973)
3. Boller, C., Chang, F.-K., Fujino, Y.: Encyclopedia of Structural Health Monitoring. John Wiley & Sons, New Jersey (2009)
4. Staszewski, W., Boller, C., Tomlinson, G.: Health Monitoring of Aerospace Structures, Smart Sensor Technologies and Signal Processing. John Wiley & Sons, New Jersey (2004)
5. Raghavan, A., Cesnik, C.E.S.: Review of guided-wave structural health monitoring. The Shock Vib. Digest. **39**, 91–114 (2007)

6. Su, Z., Ye, L., Ye, L.: Guided lamb waves for identification of damage in composite structures: a review. J. Sound Vib. **295**, 753–780 (2006)
7. Monkhouse, R.S.C., Wilcox, P.D., Cawley, P.: Flexible interdigital PVDF transducers for the generation of lamb waves in structures. Ultrasonics **35**, 489–498 (1997)
8. Giurgiutiu, V.: Structural Health Monitoring with Piezoelectric Wafer Active Sensors. Academic Press—Elsevier, Amsterdam (2008)
9. Rose, J.L.: Ultrasonic Waves in Solid Media. Cambridge University Press, Cambridge (2004)
10. Staszewski, W.J., Lee, B.C., Mallet, L., Scarpa, F.: Structural health monitoring using scanning laser vibrometry: I. Lamb wave sensing. Smart Mater. Struct. **14**(2), 251–260 (2004)
11. Nayfeh, A.L.: Wave propagation in anisotropic media, North Holland Series. In: Applied Mathematics and Mechanics, vol. 39 (1995)
12. Pohl, J., Mook, G., Szewieczek, A., Hillger, W., Schmidt, D.: Determination of lamb wave dispersion data for SHM, 5th European Workshop on Structural Health Monitoring, Italy (2010)
13. Hillger, W., Szewieczek, A.: Verfahren zur Optimierung eines Sensornetzwerks (Procedure for optimization of a sensor network). Patent No. 10 2009 019 243.3, German Patent and Trade Mark Office (2009)
14. Monkhouse, R.S.C., Wilcox, P.W., Lowe, M.J.S., Dalton, R.P., Cawley, P.: The rapid monitoring of structures using interdigital lamb wave transducers. Smart Mater. Struct. **9**, 304–309 (2000)
15. Veidt, M., Liu, T., Kitipornchai, S.: Modelling of lamb waves in composite laminated plates excited by interdigital transducers. NDT&E Int. **35**, 437–447 (2002)
16. Matthews, H.: Surface Wave Filters—Design, Construction, and Use. John Wiley & Sons, New Jersey (1977)
17. Wierach, P.: Elektromechanisches Funktionsmodul, German Patent DE 10051784 C1 (2002)